Research Square

Preprints are preliminary reports that have not undergone peer review.
They should not be considered conclusive, used to inform clinical practice,
or referenced by the media as validated information.

A leptomeningeal-astrocyte co-culture model reveals that cell communication informs barrier function and gene expression at the human pial-glial membrane

Erin C. Reardon
University of Limerick
Aisling J. Greaney
University of Limerick
Olwyn R. Mahon
University of Limerick
Mannthalah Abubaker
University of Calgary
John J. E. Mulvihill
john.mulvihill@ul.ie

University of Limerick

Research Article

Keywords: pia mater, glia limitans, leptomeninges, brain fibroblasts, barrier, rna sequencing, Transendothelial/transepithelial electrical resistivity, permeability

Posted Date: November 5th, 2026

DOI: https://doi.org/10.21203/rs.3.rs-11434655/v1

License: This work is licensed under a Creative Commons Attribution 4.0 International License.
Read Full License

Additional Declarations: No competing interests reported.

Abstract

The pial-glial membrane is a specialised interface which maintains separation between the brain parenchyma and cerebrospinal fluid, limiting immune cell entry into the brain. This structure is comprised of two dominant cell types, leptomeningeal cells and astrocytes, separated by a shared basement membrane. Despite its importance, there are few *in vitro* models which examine this brain border. This study comprehensively examines a leptomeningeal-astrocyte co-culture model through transcriptomic profiling, functional barrier assessment, and protein expression. Co-culture generates distinct, interaction-mode-dependent transcriptional states. Functional barrier assessment reveal that astrocytes are essential modulators of leptomeningeal cell barrier functions, significantly increasing transendothelial resistance while maintaining physiological permeability. Protein validation highlights challenges in identifying leptomeningeal markers *in vitro*, with all markers detected in adult human meningeal tissue including BMP5 and NGFR. Collectively, these findings establish a foundational model for dissecting pial-glial interactions, defining the global transcriptional reprogramming elicited by co-culture, and advancing mechanistic understanding of barrier function.

Introduction

The interface between the brain parenchyma and the meninges, also referred to as the pial-glial membrane, is formed by two closely apposed cellular layers: leptomeningeal cells of the pia mater and the astrocytic glia limitans (1, 2).

The pial-glial membrane forms the final critical defence protecting the brain from external insults (3, 4). The pia mater and glia limitans are permeable barriers, preventing the entry of immune cells such as T-cells into the brain (2, 3, 5). Furthermore, it also acts as a barrier to neurite growth, separating the brain parenchyma from the external cerebrospinal fluid (6–8). Damage to this interface can also lead to significant impacts in cortical development (8) and worsen outcomes in traumatic brain injury (9). Despite these essential roles, major questions remain unanswered regarding the barrier properties of leptomeningeal cells, the functional relevance of transcriptionally distinct leptomeningeal cell populations (10, 11), and the influence of astrocytes on the leptomeningeal cells (12). Although rodent studies have provided foundational insight on this brain interface (2, 5), interspecies differences in anatomy, cellular identity, and molecular signalling (10, 13) underscore the value of complementary human-based *in vitro* models.

In vitro models have been central to the progress made within the blood-brain barrier (BBB) field, allowing for a better mechanistic understanding of the cellular communication driving barrier functions (14, 15). When comparing this to the pial-glial membrane, there has been little progress made *in vitro* with limited papers looking at this interface using astrocytes and leptomeningeal cell co-culture (12). The findings from these studies can be contradictory with a focus on neurite outgrowth, limited data on protein expression, and no investigation on gene expression or barrier functions (6, 16–20). There is an evident need for an *in vitro* co-culture model of the human pial-glial membrane as there are many open questions

and controversies within meningeal biology (10). Prior to this study, there has been no suitable *in vitro* co-culture model which could mimic the pial-glial membrane to examine these interactions. As a result, key mechanistic questions including how leptomeningeal cells and astrocytes interact, how barrier properties emerge, and how cell identity is maintained, remain unanswered.

This study aims to address these gaps by developing an *in vitro* co-culture model of the pial-glial membrane (alternatively, the brain-meninges interface) using both primary human leptomeningeal cells and astrocytes. Through integrated analyses encompassing transcriptomic profiling, functional barrier assessment, and protein confirmation *in vitro* and in human tissue, this study delivers a comprehensive characterisation of the human *in vitro* model of the pial-glial membrane, which allows for an understanding of leptomeningeal-astrocyte interaction. This foundational work establishes a platform for understanding this interface and allows us to answer some of the open questions within the field (10).

Materials and Methods

This study employed transcriptomic profiling, barrier function assays, and protein expression analysis to investigate leptomeningeal–astrocyte cell interactions *in vitro*. An overview of the experimental workflow is shown in Fig. 1.

Cell culture

Primary human leptomeningeal cells (21, 22) (LMCs; #1400, ScienCell) and astrocytes (21) (ASCs; #1800, ScienCell) were cultured according to the manufacturer's recommendations. Cells were maintained in poly-L-lysine (PLL; P4707-50ML, Sigma Aldrich) coated T75 flasks at a seeding density of 5,000 cells/cm². LMCs were grown in complete meningeal medium (#1401, ScienCell), and ASCs in astrocyte medium (#1801, ScienCell), each supplemented with 1% growth supplement, 2% fetal bovine serum (FBS), and 1% Penicillin–Streptomycin. Cultures were incubated at 37°C with 5% CO_2, and media were replaced every three days until confluency. Cells were seeded at 5,000 cells/cm² for all subsequent assays unless otherwise specified.

Human Umbilical Vein Endothelial Cells (HUVECs) were cultured according to the manufacturer's recommendations. They were grown in complete Endothelial Cell Growth Medium 2 (C-22011, Sigma Aldrich) and maintained as per the LMCs and ASCs.

Co-culture seeding ratios and media for viability

LMCs and ASCs were subcultured according to supplier instructions and prepared as single cell suspensions at three ratios: 70:30, 50:50, and 30:70 (LMC:ASC). Cells were seeded onto PLL coated 96 well plates at recommended densities in five media conditions: LMC medium, ASC medium, and three mixed media formulations corresponding to the defined ratios. MTT and AlamarBlue assays were

conducted once the cells reached confluency in triplicate experiments with 6–8 technical replicates. Leptomeningeal cells in LMC medium served as the control for statistical analysis. All viability results are included in supplementary file 1, Figure S1.

MTT assay

10 µL of MTT solution was added to wells containing 100 µL medium and incubated for 4 h at 37°C, including media only wells as blanks. After removing the MTT containing medium, 100 µL DMSO was added to solubilize formazan crystals, followed by 15 min incubation with gentle agitation. Absorbance was measured at 550 nm.

AlamarBlue assay

10 µL of AlamarBlue (BUF012B, BioRad) was added to each well containing 100 µL of media, including media only wells as blanks. This was allowed incubate for 1 h in the incubator at 37 ºC and then absorbance was measured with a plate reader at wavelength 590 nm.

Cell growth analysis

A real-time cell analysis (RTCA) system (xCELLigence, Agilent Technologies Inc) was used to measure the cell growth of some of the co-culture conditions identified in the MTT/Alamar data. The RTCA system examines cell growth based on cellular impedance through Cell Index (CI) values. This is influenced by the cell attachment, cell spreading and cell proliferation. Background measurement was taken by placing 100 µL of medium into the electronic plates and acquiring a CI reading. 3–6 replicates were set up to assess the co-culture growth compared to LMC or ASC monocultures in their own complete medium. For data analysis, the B-CI (Baseline Cell Index) is determined by subtracting the CI for a cell-containing well from the CI of the blank control.

Bulk RNA sequencing sample preparation

To generate samples for bulk RNA sequencing, monocultures of LMCs and ASCs, a 30:70 LMC:ASC direct co-culture, and a Transwell co-culture (LMCs on the apical membrane; ASCs on the basolateral plate) were established (n = 4 replicates). Two independent LMC lots were used to assess culture heterogeneity, given the known diversity of LMC fibroblast subtypes within the meninges. For the Transwell co-culture, LMCs and ASCs were co-cultured until confluency, harvested individually, and then combined for sequencing.

Once the cultures were confluent the cells were pelleted and total RNA was extracted using the RNeasy Mini Kit (74104, Qiagen) following the manufacturer's protocol. Bulk RNA Sequencing was conducted by Genewiz. Briefly, the RNA samples were quantified using the Qubit Fluorometer (Life Technologies,

Carlsbad, CA, USA) and RNA integrity was checked with an RNA Kit on a Fragment Analyzer (Agilent Technologies, Palo Alto, CA, USA). RNA sequencing libraries were prepared using the NEBNext Ultra II RNA Library Prep Kit for Illumina following manufacturer's instructions (NEB, Ipswich, MA, USA). Sequencing libraries were validated using Agilent Tapestation (Agilent Technologies, Palo Alto, CA, USA), and quantified using Qubit Fluorometer (Invitrogen, Carlsbad, CA). The sequencing libraries were multiplexed and loaded on the flow cell on the Illumina NovaSeq X instrument according to manufacturer's instructions. The samples were sequenced using a 2x150 Pair-End (PE) configuration. Raw sequencing data (bcl files) generated from Illumina NovaSeq were converted into fastq files and de-multiplexed using Illumina's bcl2fastq software. Raw FASTQ files were then processed using Galaxy (23) and R studio.

Bulk RNA Sequencing Analysis:

Raw FASTQ files were then processed using Galaxy 25.0 and R studio. Briefly, the FASTQ files underwent quality checks and trimmed using Cutadapt, and files were aligned to the Hg38 reference genome using HiSAT2. Reads were sorted into feature counts using FeatureCounts. Following this, DESeq2 was used to normalise the raw counts based on read depth and perform differential gene expression analysis. For differentially expressed genes, these were taken as a log2FC > 1, and an adjusted p-value of < 0.05. Reactome was used for pathway analysis. Selected enriched Terms of interest are presented in the figures, all with an adjusted p-value of < 0.05. Supplementary files contain all the raw data obtained from differential gene expression (Supplementary File 2–5). Packages and versions used are included in the supplementary file 1, Table S1).

Transwell Co-culture:

Transwell Set-up:

0.4 µm pore Transwell polycarbonate 6 well (100–1026, Stemcell) or 12 well (140652, Thermofisher) were used to examine influence of ASCs on the LMC barrier. The Transwell plates were seeded in six different combinations to identify the optimal conditions. This included examining the LMCs alone, the LMCs with the ASCs seeded on the plate bottom, and the LMCs with ASCs seeded on the Transwell underside to find an optimal configuration. As a comparison, HUVECs, a known barrier forming cell type (24), were also cultured in the same combinations including HUVECs alone, the HUVECs with the astrocytes seeded on the plate bottom, and the HUVECs with ASCs seeded on the Transwell underside. Firstly, the ASCs were subcultured and seeded at the recommended seeding density on either the plate bottom or the underside of the Transwell. They were allowed to attach for 4–6 hours, and then the LMCs or HUVECs were seeded at the recommended density on the apical side of the Transwell. The media was refreshed every three days.

Transendothelial/Transepithelial electrical resistance (TEER)

Transendothelial/Transepithelial electrical resistance (TEER) was used to examine the barrier functions of the LMCs in the presence of absence of the ASCs, as they have been shown to improve the barrier functions of the endothelial cells in the BBB models (24, 25). TEER measurements were taken every three days using the EVOM2 (World-Precision Instruments) for 12 days, along with a measurement from a blank well – a membrane containing media but no cells. This is the background reading and was subtracted from the measured resistance values. The value acquired from each well was then multiplied by the surface area to calculate the TEER reading. Experiments were conducted in triplicate wells in triplicate experiments. TEER results ($\Omega.cm^2$) are shown as mean ± standard deviation.

Dextran

To examine the paracellular permeability, 4 kDa FITC- Dextran (46944-500mg, Sigma Aldrich) was used. Firstly, the media from the apical and basolateral sides were cleared. Fresh astrocyte media was added to the basolateral side (1.5 mL in a 12 well-plate or 2.6 mL in a 6 well-plate). Then a 1 mg/mL FITC-Dextran solution was made up in either meningeal media or Endothelial Cell Growth Medium 2.

FITC-Dextran media solution was added to each well (0.5 mL in a 12 well plate or 1.5 mL in a 6 well plate). The Transwells were incubated for 2 h at 37°C with 5% CO_2. 50 µL samples were taken from each well from the basolateral side at time 0 and every 30 min for 2 h. Sample fluorescence was measured using the microplate reader (Synergy H1, BioTek) plate reader at 490/525 nm excitation/emission. A standard curve was prepared using FITC-Dextran standard ranging from 0.005–1 mg/mL. The following formula was then used to assess the permeability of the samples. This experiment was completed with three technical replicates in three experimental replicates.

$$P = \frac{V}{A \times C_0} \times \frac{\Delta C}{\Delta t}$$

Where *P* is the permeability (cm/s), *V* is the volume of the receiving compartment (cm^2), *A* is membrane surface area (cm^2), C_0 is the initial concentration of the FITC-Dextran (1 mg/mL), ΔC is the change in concentration in the basolateral compartment (mg/mL), and Δt is the time interval (s, seconds). Permeability values were multiplied by 10^6 for ease of comparison and plotted as scaled values.

Immunofluorescence of Transwells:

LMCs and HUVECs were cultured as mentioned above, and at day 9 were fixed and stained as per the immunofluorescence protocol detailed previously. Once primary, secondary, and DAPI staining was complete, the Transwell membrane was carefully cut using a scalpel at the edges. They were carefully handled using tweezers and placed on a glass slide cell-side upwards. The coverslip was mounted on top of the membrane using a drop of ProLong™ Diamond Antifade Mountant (P36965, Invitrogen).

Immunofluorescence

Cells were fixed with 4% paraformaldehyde (PFA; 252549, Sigma Aldrich) for 15 min at room temperature, permeabilised with 0.1% Triton-X-100 in PBS for 5 min, and blocked with 5% FBS and 0.005% Triton-X-100 in PBS for 1 h. Primary antibody incubation was performed overnight at 4°C. The following day, cells were incubated with appropriate secondary antibodies for 1 h at room temperature in the dark. All primary and secondary antibodies details are included in the supplementary file 1, Table S4. Nuclei were counterstained with DAPI (D9542, Sigma Aldrich) for 10 min. Cells were washed three times with PBS between steps. Imaging was performed using an ImageXpress® Micro Confocal microscope (Molecular Devices) at 20× magnification. Images were analysed using a customised CellProfiler v4.2.4 pipeline to quantify morphology and protein intensity. All samples were imaged under identical acquisition settings to ensure reproducibility.

Representative images were processed using ImageJ v1.54f. To standardize the visual representation of fluorescence intensity across all conditions, individual images were converted to stacks to preserve the intensity values. Brightness and contrast were adjusted across all images within a stack ensuring consistent changes across all images, which better represent the intensity values.

Immunohistochemistry

Human meningeal tissue samples were obtained from the South West Dementia Brain Bank (SWDBB) (Supplementary S1, Table 2). A Material Transfer Agreement was put in place between the University of Bristol (SWDBB) and UL and ethical approval for the tissue acquisition was reviewed and approved by the Faculty of Science and Engineering Research Ethics Committee (Code: 2025_02_23_SE). Tissue was stored in RNAlater at − 80°C until use. Two independent samples were used for protein confirmation, one male and one female. Samples were thawed, fixed in 10% neutral buffered formalin (NBF) overnight, and processed using the Leica TP 1020 automated tissue processor. Tissues were embedded in paraffin using the Leica TP 1020 embedder. Tissue was sectioned at 5 µm thickness and mounted on frosted, positively charged glass slides. The slides were baked for 1 hour at 60 ºC before staining.

Immunohistochemistry was performed using the Bond Rx Fully Automated Research Stainer (Leica Biosystems) following the manufacturer's user manual. Slides were dehydrated through graded ethanol (70%, 90%, 100%, 100%) and xylene for 2 min each, then scanned at 40× using the Akoya Fusion Imager. Antibody concentrations and protocols are provided in the supplementary file 1, Table S5. Images were processed using QuPath version 0.7.0.

Statistical Analysis:

Each experimental assay included defined replicates to ensure statistical robustness and reproducibility, which are detailed here. For viability assays, 6–8 technical replicates in triplicate experiments were analysed. For immunocytochemistry imaging, three wells of a 96-well plate were seeded per condition. From each well, five randomly selected fields of view were used for statistical analysis. For TEER and permeability assays, three technical replicates in triplicate experiments were analysed. All statistical

analysis was carried out using Prism 6 software Version 10.4.1 (GraphPad, U.S.A.). All datasets were tested for normality using the Shapiro-Wilk test. For normally distributed data, values were compared using a one-way ANOVA or two-way ANOVA depending on data type. For non-parametric data sets, values were using the Kruskal-Wallis test using 95% confidence interval with Dunn's multiple comparison test. All error bars indicate standard deviation of the mean with the following asterisks for significance - ns > 0.05, * P ≤ 0.05, ** P ≤ 0.01, *** P ≤ 0.001, and **** P ≤ 0.0001.

Results

Transcriptional Signatures of Astrocyte–Leptomeningeal Monocultures and Interactions in Direct and Indirect Co-Culture

To characterise the cell types at the pial-glial membrane and assess how co-culture influences transcriptional profiles, bulk RNA sequencing was performed on two independent LMC lots (LMC1 and LMC2), astrocytes (ASC), direct co-culture (DirectCC – 30:70 LMC1:ASC ratio), and Transwell co-culture (Transwell). Principal component analysis (PCA) (Fig. 2A) revealed clear separation between major cell groups and highlighted the pronounced transcriptional heterogeneity between LMC1 and LMC2. The co-culture groups clustered between the ASC and LMC1 monoculture conditions, consistent with an intermediate transcriptional profile comprising contributions from both cell populations. This is further illustrated in the sample distance analysis plot (Fig. 2B) and heatmap (Fig. 2C). LMC1 and LMC2 have many shared transcriptional features, however, the heatmap also highlights the considerable differences in gene expression. Notably, both co-culture conditions lead to a global change in gene expression (Fig. 2C) compared to LMC1 and ASC monocultures. While these differences may partly reflect the combined transcriptional contributions of the two cell populations, they may also indicate transcriptional changes associated with co-culture. This suggests that the LMC-ASC *in vitro* co-culture model captures gene-expression programmes arising from interactions between the two cell types, potentially through direct contact or indirect signalling.

Bulk RNA sequencing Reveals Leptomeningeal Cell Diversity

Bulk RNA sequencing revealed two transcriptionally distinct LMC subtypes, LMC1 and LMC2 (Fig. 2A), consistent with the growing literature of diverse fibroblast populations within the meninges (11, 26, 27). This finding highlights the heterogeneity of commercially sourced primary cells due to donor variability. Further detailed analysis of our bulk RNA supported this diversity of the LMCs. Figure 3A shows the volcano plot of differentially expressed genes (log2FC > 1, padj < 0.05) between LMC1 and LMC2, strongly supporting the presence of two transcriptionally different leptomeningeal populations in our cultures with 1,516 genes significantly up regulated in LMC1 and 1,804 genes in LMC2. The large number of differentially expressed genes suggests that the distinction between LMC1 and LMC2 extends beyond

variation in a small number of markers and instead reflects broader differences in their transcriptional programmes. Further characterisation of these differentially expressed genes was therefore performed to determine the biological processes and cellular functions distinguishing the two LMC populations.

Reactome analysis revealed several enriched biological processes distinguishing LMC1 from LMC2 (Fig. 3B). Enrichment highlighted a cohesive collection of pathways relating to extracellular matrix organisation and formation, Wnt signalling, and retinoic acid signalling within LMC1. Whereas LMC2 is enriched for various immune signalling pathways including IL-10, and interferon signalling. This data suggests that LMC1 and LMC2 are not only transcriptionally different but differ in biological states and functions.

Furthermore, we show that LMC1 is enriched with genes associated with neurodevelopment and corticogenesis such as *Foxc1, Corin*, and *Foxp2*, basement membrane components including *Vcan* and *Nid1*, and retinoic signalling including *Aldh1a1, Crabp2*, and *Stra6*. LMC2 also shows high expression of certain ECM related genes such as *Lum, Vtn*, and *Col6a1*, expression of desmosomes and cytokeratins including *Dsg2, Krt8*, and *Krt18* which is expected in leptomeningeal cells (22). *Pecam1, Cdh5*, and *Lyve1* are also enriched in LMC2 which is associated with an endothelial and lymphatic cell type (Fig. 3C).

To create a representative *in vitro* co-culture model of the pial-glial membrane, layer specific markers were examined to characterise and annotate LMC1 and LMC2. As no single marker reliably distinguishes pial from arachnoidal LMCs across mouse, human, and *in vitro* models, a panel of commonly used markers was selected (Fig. 3D). LMC1 shows a pial phenotype with high expression of *Bmp5, Ngfr, Apod, Itih5, Lama2*, and *Lama3* (11, 28, 29). However, LMC1 also has high expression of certain arachnoid markers such as *Crabp2* and *Alcam* (11). LMC2 does not express a clear pial or arachnoidal signature, however, shows high expression for the leptomeningeal cell markers *Pdgfra, Icam1, Slc38a2*, and the arachnoidal markers *Dpp4, Aldh1a2*, and *Ptgds* (11, 30). Therefore, this expression profile is indicative of a leptomeningeal cell population which is lacking a layer-specific identity. LMC1, due to its high expression of several pial markers, represents the more suitable cell type for modelling the pial-glial membrane and is used for further comparison and co-culture.

Differential Expression Analysis Reveals Distinct Signalling Programs and Marker Candidates Between LMC1 and Astrocytes

We next examine the differential gene expression between LMC1 pial-like cells and astrocytes to define their transcriptional profiles in monoculture. This analysis aimed to characterise the molecular differences between the two cell populations, identify signalling ligands and receptors that may contribute to LMC-ASC communication, and identify candidate markers to distinguish the cell types when used in the *in vitro* co-culture model. Differential expression analysis identified 2,032 genes significantly upregulated in LMC1 and 2,076 genes significantly downregulated in astrocytes ($log2FC > 1$, $padj < 0.05$) (Fig. 4A).

Reactome analysis revealed distinct enriched pathways in the ASCs and LMC1 (Fig. 4B), whereby LMC1 is enriched for retinoic acid signalling and synthesis, whereas ASCs are enriched for ECM organisation, gap junction assembly, and *Sema3a* signalling. Given the established role of semaphorin signalling in LMC-ASCs communication, we next examined this in more detail, along with commonly known LMC and ASC ligand and receptors. (Fig. 4C).

Overall, LMC1 was characterised by enrichment of ephrins (*Efnb3*, *Efna5*), BMPs (*Bmp5, Bmp6*), and PDGFs (*Pdgfd, Pdgfb*) family signalling components, whereas ASC showed preferential expression of *Wnt7b*, *Sema3a*, *Pdgfc*, and VEGFs (*Vegfc, Vegfa*) family ligands, suggesting divergent paracrine signalling between the two cell populations.

A key challenge in establishing an LMC-ASC *in vitro* co-culture model is the ability to reliably distinguish the two cell populations, due to the lack of suitable cell-specific markers. Therefore, using commonly used ASC and LMC markers, Fig. 4D examines the expression of these in each cell type with *Bmp5, Ngfr, Acta2*, and *Crabp2* showed the strongest differential expression in LMC1 relative to ASCs, highlighting their potential utility as markers for identifying LMCs within the co-culture model.

Indirect Co-culture Elicits More Pronounced Transcriptional Responses Than Direct Contact

To model the pial-glial membrane using primary human ASCs and LMCs, we established two complimentary co-culture approaches, – direct and indirect. Our initial transcriptional analysis demonstrated that co-culture led to a distinct transcriptional state, different from monoculture, and not just a combination of two cell types (Fig. 2A). While this profile likely reflects, in part, the combined transcriptional contributions of both cell populations, it may also capture transcriptional changes arising from LMC–ASC interactions (Fig. 2A).

Importantly, the transcriptional differences observed under co-culture conditions were unlikely to reflect compromised cell viability or suboptimal culture conditions, as the cell-cell ratios and cell medias were tested using viability, metabolic, and real-time cell analysis to ensure stable conditions for both cell types prior to co-culture experiments (Supplementary File 1, Figure S1). To further examine the influence of co-culture of these cells on gene expression, LMC1 and the ASCs were pooled into a monoculture group and compared to both the direct co-culture and Transwell co-culture (Fig. 5A). DirectCC yielded a comparatively modest transcriptional response, with 164 DEGs identified, whereas Transwell co-culture induced upregulation of a substantially larger gene set (974 genes). Despite this difference, only 80 genes were shared between the two conditions, representing ~ 50% of the DirectCC DEG set but only ~ 8% of the Transwell-upregulated genes (Fig. 5B).

Co-culture led to the increase of various cadherins such as *Cdh1, Cdh8, Cdh7*, and *Cdh23* along with *Shh* and *Gpr37L1* which are associated with neurodevelopment and astrocyte maturation respectively. Across these genes, there is a more pronounced effect within the Transwell group than the DirectCC

group, highlighting that direct contact between the cells may not be required for these transcriptional changes. In Fig. 4D, several LMC markers were identified, and Fig. 5C shows if their expression differs when in co-culture. There are variable results with *Ngfr* increasing in Transwell, whereas *Crabp2* is reduced in both co-culture conditions, displaying a challenge of suitable *in vitro* markers.

Pathway analysis revealed Transwell had a much more pronounced enrichment of biological processes compared to DirectCC. These included extracellular matrix, sema3a signalling, gap junction assembly, and retinoic acid signalling. Overall, these pathways have been found in the ASC versus LMC Reactome analysis in Fig. 5D. This is interesting as Transwell co-culture leads to an enrichment of these pathways, whereas DirectCC does not, emphasizing the effect of paracrine signalling rather than direct contact, and maintenance of ASC and LMC functions within co-culture. DirectCC led to an enrichment of interleukin 7 signalling which is associated with the neural (31) and B cell development (32).

Astrocytes Improve the Barrier Functions of Leptomeningeal Cells

The effect of co-culture of LMCs with ASCs to improve the barrier formation was examined by taking TEER measurements every three days over 12 days in the Transwell co-culture model. There is a significant increase in TEER values when LMCs were cultured in the presence of ASCs, with no notable difference between the apical (LMC + ASC (u)) and basolateral (LMC + ASC (b)) seeding configurations. The highest TEER value of the LMCs was recorded at day 9 reaching 99.98 Ohms.cm^2, nearly double the LMC only group at 55.24 Ohms.cm^2 (Fig. 6A). By day 12, the barrier functions start to decline which is due to cell death as the cells have overgrown. Next, barrier permeability was assessed using 4 kDa FITC-Dextran. Permeability measurements were taken in the matching combinations and timepoints as per the TEER data, examining the influence on ASCs on the LMCs. Overall, there is no significant difference between the conditions (Fig. 6B), however, there is a trend in the reduction of permeability when co-cultured.

As the barrier functions of the LMCs are understudied, HUVECs, an endothelial cell line commonly used to model the BBB (33), were used as a comparison. Day 12 readings were not taken for the HUVECs as they were completely overgrown by this time, precluding reliable measurements at this timepoint. Overall, at day 9, the presence of ASCs has a significant effect on the barrier functions of the HUVECs (Fig. 6C). However, similar to the LMC cultures, this change was not accompanied by a change in permeability (Fig. 6D).

Finally, VE-cadherin localisation in the LMCs in the presence and absence of ASCs was examined (Fig. 7A). VE-cadherin is a key component of adherens junctions and is the most commonly used marker for meningeal barriers (5). As barrier integrity depends on the organisation and localisation of junctional proteins at cell–cell contacts, VE-cadherin distribution was assessed as a complementary measure of LMC barrier organisation alongside TEER and permeability. VE-cadherin is localised to the nucleus in the LMCs, which has been reported in other cell types and experimental contexts (34, 35). There is no

change to the localisation pattern of VE-cadherin in the presence of ASCs, suggesting that the observed changes in barrier function are unlikely to be explained by redistribution of VE-cadherin. Therefore, there may be other junctional and adherin proteins, identified in the transcriptional analysis (Fig. 5), may be contributing to these co-culture-associated changes in LMC barrier functions.

The presence of ASCs significantly increased the electrical resistance in both LMCs and HUVECs in comparison to monoculture controls. When comparing across the LMCs and HUVECs, the LMC + ASC (b) has no significant difference in TEER with the HUVECs only (Fig. 7B). As HUVECs are a cell line used for their barrier functions and junctional protein expression (36), this highlights the importance of astrocytes in improving the LMCs barrier functions to a physiologically relevant barrier. However, differences between the LMC and HUVEC barrier phenotypes became more apparent in the permeability assay, with HUVECs exhibiting significantly lower dextran permeability than either LMC monoculture or LMC–astrocyte co-culture (Fig. 7B–C). This is expected as 4 kDa FITC-Dextran is only restricted in barriers with strong junctions such as the BBB. The pial-glial membrane is a permeable barrier, allowing for the passage of 3–10 kDa tracers (2, 5). Nonetheless, a significant reduction in permeability over time was observed, indicating progressive barrier maturation.

Together these findings demonstrate that ASCs are essential for establishing a functional *in vitro* model of the pial-glial membrane with significantly enhanced barrier functions with mimetic permeability functions as *in vivo*.

Protein-Level Characterisation of Leptomeningeal and Astrocyte Identity Markers

A panel of candidate markers were selected for validation at the protein level using immunocytochemistry across the four experimental conditions which allows us to understand the LMC heterogeneity and investigate if there is a cell-specific protein which can differentiate the LMCs from ASCs in DirectCC.

The markers selected includes Bone Morphogenetic Protein 5 (BMP5), p75 neurotrophin receptor (NGFR/p75NTR), Cellular retinoic acid-binding protein 2 (CRABP2), Fibronectin (FN1), Vascular endothelial cadherin (VE-cadherin), and Alpha-smooth muscle actin (ACTA2/α-SMA). To assess potential overlap between LMCs and ASC populations within co-culture systems, established astrocyte markers Glial fibrillary acidic protein (GFAP) and S100 calcium-binding protein B (S100B) were examined. More detail on the roles of these proteins is included in the supplementary file 1, Table S4.

BMP5 emerged from our bulk RNA-sequencing analysis as a strongly enriched transcript in the pial-like LMC1 subtype. Immunocytochemistry confirmed this at the protein level: BMP5 expression was significantly higher in LMC1 than in LMC2, however no difference was observed between LMC1 and astrocytes (Fig. 8). Notably, BMP5 displayed distinct nuclear localisation within LMC1. NGFR, a receptor protein and often used as a pial marker within mice and fetal human dataset (11),was shown to have diffuse staining across all conditions, with only certain cells in each condition strongly staining. Overall,

LMC1 shows certain cells with pronounced staining, and LMC2 shows diffuse staining across the cells which contributes to its higher expression. CRABP2 is often used as an arachnoidal marker (11), however, expression was observed within all conditions. Taken together, the overlapping expression of pial cells and arachnoidal-associated markers suggests that the LMC cultures do not represent a single, clearly defined leptomeningeal subtype, but rather comprises a heterogenous population.

Interestingly we show that both ASCs and LMC1 stained strongly, indicated by mean intensity values, for fibronectin, which is often used a marker to differentiate ASCs and LMCs (Fig. 8). However, LMC2 has low expression of fibronectin, which was unexpected. Furthermore, the co-culture of LMC1 and ASCs show fibronectin deposition rather than expression within the cells, which contributes to the overall lower mean intensity. This questions if fibronectin is a suitable marker for LMCs if there is also high expression within astrocytes *in vitro* (37–39).

VE-cadherin expression was significantly higher in LMC2 compared to LMC1. However, VE-cadherin is localised primarily to the nucleus within all conditions and not at the cell-cell junctions. Co-culture of LMC1 and ASC led to a significant increase in VE-cadherin mean intensity, however, with no localisation to the cell junctions. ACTA2 is used as a mural marker within the meninges (40) and shows high expression within the LMC2 and ASCs. There is much lower expression within LMC1, suggesting a more leptomeningeal phenotype in these cells. Differences in fluorescence intensity and apparent subcellular distribution were observed across conditions, however, none of the candidates reliably distinguished LMCs from ASCs in direct co-culture, highlighting the challenges of using these well-known markers at the protein level *in vitro*.

Furthermore, GFAP and S100B expression was examined across the conditions, which are commonly used astrocyte markers. There is little expression of GFAP within our primary human ASCS which is expected based on the literature (41, 42). Figure 9 shows the positive astrocytes within the ASC and DirectCC conditions, with a complete absence in LMC1 and LMC2. S100B is often used as an astrocyte marker, however, was also expressed in our LMCs as shown in Fig. 9. This highlights another challenge with using GFAP as an astrocyte marker rather than a marker of astrocyte reactivity, and the challenges in identifying a marker which can differentiate between the LMCs and ASCs.

Conservation of Candidate Markers in Adult Human Meninges

To determine whether candidate proteins identified in the *in vitro* model are also expressed in adult human meninges, immunohistochemistry was conducted on human meningeal tissue. This is particularly important as some of these proteins have not previously been identified at the protein level within human meningeal tissue or have not shown to be conserved into adulthood. Using two adult samples, six proteins were confirmed in meningeal tissue, with all proteins being expressed (Fig. 10), supporting the conservation of their expression into adulthood. However, it must be noted that while

these findings confirm their presence in adult human tissue, they still do not establish their ability to distinguish between leptomeningeal cell populations *in vitro*.

BMP5 has been shown to be expressed in fetal human tissue (11), however, has never been shown to be retained in adult human tissue. Here, we show that BMP5 expression is retained at the protein level into adulthood. Both our pial marker, NGFR, and arachnoidal marker, CRABP2, exhibited widespread and high expression within the meninges, showing the presence of leptomeningeal cells in the tissue. As expected, fibronectin, VE-Cadherin, and ACTA2 are widely expressed within the meninges. ACTA2 is highly expressed around the vessels within the meninges which supports our claim that our LMC2 may have a more mural phenotype.

Discussion

A recent systematic review of the literature using co-culture of astrocytes and leptomeningeal cells highlighted many gaps in the knowledge and an overall lack of *in vitro* models that recapitulate pial-glial membrane or brain-meninges interface (12). This study provides the most comprehensive analyses to date of an *in vitro* co-culture model of the pial-glial membrane using primary human leptomeningeal cells and astrocytes analysing transcriptomic profile, protein expression, and barrier functions.

Transcriptomic analysis of the *in vitro* co-culture model displayed a distinct transcriptional state compared to monoculture controls, which cannot be accounted for by the combination of the two cell types. Additionally, two transcriptionally distinct leptomeningeal cell types were identified within this study, highlighting the importance of carefully characterising the cell type for *in vitro* model use. Given the significant leptomeningeal cell heterogeneity within the meninges (11), distinct populations may exhibit different functional properties and should therefore be considered when selecting cells for model development. We show that LMC1 has a pial phenotype with high expression of *Bmp5, Ngfr*, and *Apod* (11, 29), whereas LMC2 does not show a clean layer specificity. Furthermore, LMC1 has high expression of many genes which is associated with early neurodevelopment such as *Cxcl12*, *Foxc2*, and *Zic* family members (Supplementary File 2) (43). This was highlighted in the Reactome analysis where LMC1 had enrichment in retinoic acid signalling (44, 45) extracellular matrix development (46), and Wnt-signalling. Pial cells in fetal mouse studies have been shown to be enriched in *Bmp5* in the posterior located meninges. Moreover, retinoic acid signalling has been shown to have differential gene expression within the pial versus arachnoidal cells (11). This same pattern is seen within our LMC1 phenotype, supporting our annotation of this cell type as a pial-like leptomeningeal cell. These cells could be a useful model for studying how retinoic acid signalling from the meninges can influence cortical development (45) in fetal human neurodevelopment or in the development of the glia limitans (4, 47). LMC2 had a more immune (48) and vascular associated phenotype (49) which may be more suitable for modelling the subarachnoid space which is highly vascularised. As this study focuses on the development of an *in vitro* co-culture model of the pial-glial membrane, it is important to include the correct leptomeningeal cell type, therefore LMC1 was used for further co-culture studies.

Prior to co-culture the leptomeningeal cells and astrocytes, the transcriptomic profile of the cells was characterised independently in monoculture. Astrocytes showed enrichment of various astrocyte markers such as *Slc13a3, Sox2*, and *Fabp7.* These genes are important genes in astrocyte maturation, function, and *Fabp7* has been shown to be upregulated in astrocytes within the glia limitans (4, 44, 50). Leptomeningeal-astrocyte interaction has been examined in many papers with important roles of semaphorins, ephrins, BMPs, in both *in vitro* and transcriptomic work (29, 51–53). Taking the learnings from (29) and their transcriptomic analysis of ligand-receptor interactions within leptomeningeal cells and astrocytes, we examined this within our study. We showed high expression of several of the genes across both cell types, although their relative expression differed between leptomeningeal cells and astrocytes, demonstrating distinct cell type–specific expression profiles. This includes BMPs within the leptomeningeal cells and Sema3a in the astrocytes. Reactome analysis further highlighted *Sema3a* signalling and axon repulsion within astrocytes (6, 53), along with roles in extracellular matrix, and gap junction assembly, whereas retinoic acid signalling was again enriched in LMC1. This allows us to understand the biological function of the cells prior to co-culture and opens for further molecular analysis of ligand-receptor signalling between these cell types to understand their cell communication.

We demonstrate that co-culture of leptomeningeal cells and astrocytes does not simply combine two cell types but leads to a distinct transcriptional state which is interaction dependent. Comparing direct and Transwell co-culture revealed that indirect interactions exert a substantially stronger transcriptional influence. Transwell co-culture resulted in 974 differentially expressed genes relative to monoculture, whereas direct co-culture produced only 164 upregulated genes, with only 80 shared genes between them. This suggests that secreted factors, rather than physical contact, drive the most transcriptional changes. There were significant increases in the expression of cadherins and integrins, particularly in the Transwell condition, including *Cdh1, Cdh8, Cdh23, and Itga8*, which may be contributing to the increase in barrier functions (54, 55) and formation of this permeable barrier at the pial-glial membrane. *Gpr371l* and *Shh*, genes involved in astrocyte maturation and corticogenesis, were also upregulated in co-culture (50, 56) which suggests a bi-directional communication between both the leptomeningeal cells and astrocytes. This is reflected in the Reactome analysis which highlighted enrichment of extracellular matrix organisation, *Sema3a* signalling with axon repulsion, and retinoic acid signalling (6, 11, 57). Overall, this transcriptional profile supports the *in vitro* co-culture model recapitulates key biological programs and global gene expression associated with the pial-glial membrane, supporting its use as a physiologically relevant mimetic model of this interface.

This is the first study to report the influence of astrocytes on the leptomeningeal cell barrier functions. We found a significant increase in the TEER values in the presence of astrocytes, along with a reduction in permeability. This data matches well with the literature, showing that the pia and glia limitans is permeable to 3–10 kDa dextran (2, 5). From our data, we can see there is no localisation of VE-cadherin to the cell junctions in the LMCs unlike in the HUVECs. As suggested, the predominant nuclear localisation in LMCs may reflect the absence of specific cues within the environment, required for its appropriate junctional localisation. Moreover, we can suggest that this increase in barrier function may instead be due to a combination of gene expression changes such as *Cdh1, Cdh8, Cdh23*, and *Itga8*,

which were identified in the sequencing data. This study highlights the essential role of astrocytes on leptomeningeal cell barrier functions which mimics the pial-glial membrane. This could be used as a tool to understand the barrier function of various leptomeningeal cell types and barrier dysfunction which could address many gaps in our understanding.

Within the field of meningeal biology, transcriptomic studies have been able to identify layer-specific markers for the different leptomeningeal fibroblast populations. However, there has been little research in the *in vitro* modelling of the meninges, and the pial-glial membrane (12). There is still a challenge within this field regarding suitable protein markers which can translate across species and from tissue sections to *in vitro* cultures. This is further highlighted in Figs. 7–9, which demonstrate that commonly used markers used in mouse and human tissue may not translate reliably to *in vitro* models. For examples, fibronectin or ECM proteins have been used to differentiate the leptomeningeal cells from astrocytes (58), however, their discriminatory value in vitro may be limited and unsuitable. Similarly, GFAP has been shown to be expressed at different levels dependent on the brain region, age, and disease state (42, 59). Furthermore, in primary human cultures of astrocytes, GFAP expression can be low or absent (41) depending on the cortical region, species, or disease state, limiting its utility as a definitive marker of astrocyte cells in vitro. Our data also supports this as there is low expression of GFAP at the gene and protein level. Further work is required to address these limitations and consolidate suitable protein markers which are conserved and translate to *in vitro*. In tissue, many markers are suitable to differentiate the leptomeninges from the brain parenchyma such as NGFR and CRABP2 (11). However, these have never been identified before in an *in vitro* co-culture model of the brain-meninges interface and our findings demonstrate that these markers do not retain sufficient cell-type specificity to differentiate LMCs from ASCs, highlighting the need for markers validated specifically for *in vitro* models.

To the authors knowledge, this is the first demonstration of NGFR and BMP5 protein expression in the human adult meninges for. Although these markers have been identified within fetal mouse (11), and within transcriptomics datasets their expression has not been shown to be conserved at the protein level in adult human tissue or *in vitro* culture of human leptomeningeal cells. While BMP5 expression has been shown in pial cells and is thought to have roles in neurodevelopment and corticogenesis (11, 60–62), its function in the adult brain still remains largely unknown (63). The presence of these shared proteins between the fetal cells and the adult tissue further suggests that aspects of the molecular phenotype identified *in vitro* are maintained in the adult meninges. Together, these findings support the biological relevance of our *in vitro* leptomeningeal cells and ability to capture features of the human meningeal phenotype. While there is excellent transcriptomic work has attempted to advance the molecular characterisation of the human meninges (28, 40, 64, 65), comparatively less is known about how these transcriptional profiles translate to protein expression and function. Further work on the proteomic characterisation of the meninges is therefore required to validate emerging cell-type-specific markers and elucidate the functional roles of these proteins (66). Such studies will also be important for establishing robust molecular benchmarks against which the physiological relevance of *in vitro* models can be assessed.

Limitations:

There are several limitations within this study which should be highlighted. First, the use of commercially sourced primary human cells introduces variability related to donor age and tissue origin. However, this may be considered as an advantage, as we were able to obtain a pial-leptomeningeal cell type which was suitable for our application. Nevertheless, this emphasizes the importance of appropriate characterisation of cell types for use in an *in vitro* model. Due to the unexpected heterogeneity of the two LMC subtypes, this reduced our sample size when comparing the LMC subtypes. Increasing the sample size could improve the power of this experiment and unveil further interesting gene expression changes. The leptomeningeal cells and astrocytes used in this study were fetal in origin however, the markers identified were validated in aged-adult human patients. However, we believe this is an interesting insight as it shows the markers are conserved from fetal cells into adulthood. Furthermore, due to the type of meningeal tissue samples obtained, we are unable to specifically annotate the meningeal layers using our markers and this warrants further exploration.

Future work:

Future work should focus on increasing the complexity of this model to better recapitulate the pial-glial membrane. Incorporating physiologically relevant substrate stiffness, CSF-like flow dynamics, and additional cell types, including immune cells, will be essential for developing a more complete system and better capture the complexity of this interface/barrier (21, 32, 67, 68). Furthermore, this work could also be conducted using adult leptomeningeal cells and astrocytes, or iPSC-derived astrocytes (42) which may improve the relevancy if using this model to study age-related and neurodegenerative diseases such as Alzheimer's disease. Currently, the absence of established protocols for the generation of leptomeningeal cell iPSCs currently limits the progress of an iPSC-derived pial-glial model (47). Moreover, the field would benefit from systematic validation of cell-type-specific markers which span human tissue, rodent models, and *in vitro* cultures, enabling more reliable identification of leptomeningeal and astrocyte subtypes across experimental platforms, and ultimately, for developing more robust and physiologically relevant models of the human brain–meninges interface.

Conclusion

Overall, this study is the first to comprehensively characterise a primary leptomeningeal cell-astrocyte *in vitro* co-culture model of the pial-glial membrane. Co-culture of these cells leads to global gene expression changes and enhances the leptomeningeal cell barrier functions, demonstrating that cellular interactions are critical for establishing an *in vitro* model that is functionally and transcriptionally mimetic of the pial-glial membrane. Importantly, this study establishes a biologically relevant and experimentally tractable model of the human pial–glial membrane and will allow the field to compliment *in vivo* and human studies with *in vitro* testing to expand our knowledge and enable mechanistic investigation of this understudied interface and brain barrier.

Declarations

Acknowledgements

We would like to thank the South West Dementia Brain Bank (SWDBB), their donors and donor's families for donating brain tissue for this study. Tissue for this study was provided with support from the BDR programme, jointly funded by Alzheimer's Research UK and Alzheimer's Society, and BRACE. We thank Aoife Hennessy for training and support for immunohistochemistry using the Bond Rx Fully Automated Research Stainer. We also thank Dr. Amira Mahdi for use of the automated tissue processor and embedder at the Graduate Entry Medical School in the University of Limerick.

Resource availability

Lead Contact

Requests for further information and resources should be directed to the lead contact (john.mulvihill@ul.ie).

Materials Availability

This study did not generate new unique reagents.

Data and Code availability

- All data reported in this paper will be shared by the lead contact upon request.
- This paper does not report original code.
- Any additional information required to reanalyse the data reported in this paper is available from the lead contact upon request.

Author contributions

Conceptualization: E.R and J.M.; methodology: E.R., A.G, O.M; data curation: E.R; funding acquisition: J.M.; supervision: J.M.; writing–original draft: E.R. and J.M.; writing–review and editing: E.R., J.M., M.A., O.M.

Funding

This work was supported by Science Foundation Ireland 18/EPSRC-CDT/3583.

Declaration of interests

The authors declare no competing interests.

Ethics and Consent to Participate declarations

Not applicable

Declaration of generative AI and AI-assisted technologies in the writing process

During the preparation of this work, the authors used Microsoft Copilot to improve readability and language. After using this tool, the authors reviewed and edited the content as needed and takes full responsibility for the content of the publication.

References

1. Morris AWJ, Sharp MM, Albargothy NJ, Fernandes R, Hawkes CA, Verma A, et al. Vascular basement membranes as pathways for the passage of fluid into and out of the brain. Acta Neuropathol. 2016;131:725–36.
2. Hélie-Legoupil P, Kloster F, Pareja J, Vladymyrov M, Mapunda JA, Bouillet E, et al. In vivo imaging of the barrier properties of the glia limitans during health and neuroinflammation. Nat Commun. 2025;16(1):8895.
3. Engelhardt B, Coisne C. Fluids and barriers of the CNS establish immune privilege by confining immune surveillance to a two-walled castle moat surrounding the CNS castle. Fluids Barriers CNS. 2011;8(1):4.
4. Hasel P, Cooper ML, Marchildon AE, Rufen-Blanchette U, Kim RD, Ma TC et al. Defining the molecular identity and morphology of glia limitans superficialis astrocytes in vertebrates. Cell Rep. 2025;44 (3).
5. Mapunda JA, Pareja J, Vladymyrov M, Bouillet E, Hélie P, Pleskač P, et al. VE-cadherin in arachnoid and pia mater cells serves as a suitable landmark for in vivo imaging of CNS immune surveillance and inflammation. Nat Commun. 2023;14(1):5837.
6. Shearer MC, Niclou SP, Brown D, Asher RA, Holtmaat AJGD, Levine JM, et al. The astrocyte/meningeal cell interface is a barrier to neurite outgrowth which can be overcome by manipulation of inhibitory molecules or axonal signalling pathways. Mol Cell Neurosci. 2003;24(4):913–25.
7. Shearer MC, Fawcett JW. The astrocyte/meningeal cell interface–a barrier to successful nerve regeneration? Cell Tissue Res. 2001;305:267–73.
8. Halfter W, Dong S, Yip Y-P, Willem M, Mayer U. A critical function of the pial basement membrane in cortical histogenesis. J Neurosci. 2002;22(14):6029–40.
9. Mason HD, Johnson AM, Mihelson NA, Mastorakos P, McGavern DB. Glia limitans superficialis oxidation and breakdown promote cortical cell death after repetitive head injury. JCI insight. 2021;6 (19).
10. Betsholtz C, Engelhardt B, Koh GY, McDonald DM, Proulx ST, Siegenthaler J. Advances and controversies in meningeal biology. Nat Neurosci. 2024:1–17.

11. DeSisto J, O'Rourke R, Jones HE, Pawlikowski B, Malek AD, Bonney S, et al. Single-cell transcriptomic analyses of the developing meninges reveal meningeal fibroblast diversity and function. Dev Cell. 2020;54(1):43–59.
12. Reardon EC, Greaney AJ, Mulvihill JJE. From glia limitans to glial scars: in vitro co-culture studies of the astrocyte and meningeal interaction. Fluids Barriers CNS. 2025;22(1):103.
13. Götz J, Bodea L-G, Goedert M. Rodent models for Alzheimer disease. Nat Rev Neurosci. 2018;19(10):583–98.
14. Williams-Medina A, Deblock M, Janigro D. vitro models of the blood–brain barrier: tools in translational medicine. Front Med Technol. 2021;2:623950.
15. Cecchelli R, Berezowski V, Lundquist S, Culot M, Renftel M, Dehouck M-P, et al. Modelling of the blood–brain barrier in drug discovery and development. Nat Rev Drug Discovery. 2007;6(8):650–61.
16. Anders JJ, Salopek M. Meningeal cells increase in vitro astrocytic gap junctional communication as measured by fluorescence recovery after laser photobleaching. J Neurocytol. 1989;18(2):257–64.
17. Abnet K, Fawcett JW, Dunnett SB. Interactions between meningeal cells and astrocytes in vivo and in vitro. Dev Brain Res. 1991;59(2):187–96.
18. Struckhoff G. Cocultures of meningeal and astrocytic cells—A model for the formation of the glial-limiting membrane. Int J Dev Neurosci. 1995;13(6):595–606.
19. Grafstein B, Liu S, Cotrina ML, Goldman SA, Nedergaard M. Meningeal cells can communicate with astrocytes by calcium signaling. Ann Neurol. 2000;47(1):18–25.
20. Fujimori K, Watanabe M, Urade Y, Ishikawa K. Increased production of lipocalin-type prostaglandin D synthase in leptomeningeal cells through contact with astrocytes. Neurosci Lett. 2007;423(2):133–7.
21. Greaney AJ, Abubaker M, McCarthy CM, Reardon EC, Mulvihill JJE. Mechanical contrast between brain and leptomeninges: Insights into leptomeningeal cell and astrocyte responses to mechanical stiffness alterations. Acta Biomater. 2025.
22. Abubaker M, Greaney A, Newport D, Mulvihill JJE. Characterization of primary human leptomeningeal cells in 2D culture. Heliyon. 2024.
23. Galaxy for. accessible, reproducible, and collaborative data analyses: 2026 update. Nucleic Acids Res. 2026:gkag469.
24. Abbott NJ. Astrocyte–endothelial interactions and blood–brain barrier permeability. J Anat. 2002;200(5):523–34.
25. Kim W, Kim J, Lee S-Y, Kim H-M, Joo KM, Nam D-H. Simplified in vitro 3D co-culture-based blood-brain barrier model using transwell. Biochem Biophys Res Commun. 2022;620:63–8.
26. Derk J, Jones HE, Como C, Pawlikowski B, Siegenthaler JA. Living on the edge of the CNS: meninges cell diversity in health and disease. Front Cell Neurosci. 2021;15:703944.
27. Degenhard T, Groh AMR, Afanasiev E, Luo M, Yaqubi M, Stratton JA et al. An integrative layer-resolved atlas of the adult human meninges. bioRxiv. 2024:2024–11.

28. Sun L, Liu P, Guo J, Fang C, Li L, Liu Y et al. Deciphering the temporal transcriptional landscape of human fetal leptomeninges. Brain. 2024:awae397.
29. Ebert SN, Eisner C, Karamboulas K, Bernier L-P, Kaplan DR, MacVicar BA et al. Single cell approaches define the murine leptomeninges: cortical brain interface as a distinct cellular neighborhood comprised of neural and nonneural cell types. bioRxiv. 2025:2025–01.
30. Remsik J, Saadeh F, Tong X, Li MJ, Snyder J, Bale T, et al. Characterization, isolation, and in vitro culture of leptomeningeal fibroblasts. J Neuroimmunol. 2021;361:577727.
31. Moors M, Vudattu NK, Abel J, Krämer U, Rane L, Ulfig N, et al. Interleukin-7 (IL-7) and IL-7 splice variants affect differentiation of human neural progenitor cells. Genes Immun. 2010;11(1):11–20.
32. Mokbel AY, Burns MP, Main BS. The contribution of the meningeal immune interface to neuroinflammation in traumatic brain injury. J Neuroinflamm. 2024;21(1):135.
33. Zhao N, Guo Z, Kulkarni S, Norman D, Zhang S, Chung TD, et al. Engineering the human blood–brain barrier at the capillary scale using a double-templating technique. Adv Funct Mater. 2022;32(30):2110289.
34. Ma J, Liu T, Dong X. Advanced glycation end products of bovine serum albumin-induced endothelial-to-mesenchymal transition in cultured human and monkey endothelial cells via protein kinase B signaling cascades. Mol Vis. 2010;16:2669.
35. Rezaei M, Martins Cavaco AC, Stehling M, Nottebaum A, Brockhaus K, Caliandro MF, et al. Extracellular vesicle transfer from endothelial cells drives VE-cadherin expression in breast cancer cells, thereby causing heterotypic cell contacts. Cancers. 2020;12(8):2138.
36. McRae M, LaFratta LM, Nguyen BM, Paris JJ, Hauser KF, Conway DE. Characterization of cell-cell junction changes associated with the formation of a strong endothelial barrier. Tissue Barriers. 2018;6(1):e1405774.
37. Mpoyi EN, Cantini M, Sin YY, Fleming L, Zhou DW, Costell M, et al. Material-driven fibronectin assembly rescues matrix defects due to mutations in collagen IV in fibroblasts. Biomaterials. 2020;252:120090.
38. Mahler M, Ben-Ari Y, Represa A. Differential expression of fibronectin, tenascin-C and NCAMs in cultured hippocampal astrocytes activated by kainate, bacterial lipopolysaccharide or basic fibroblast growth factor. Brain Res. 1997;775(1–2):63–73.
39. Liesi P, Kirkwood T, Vaheri A. Fibronectin is expressed by astrocytes cultured from embryonic and early postnatal rat brain. Exp Cell Res. 1986;163(1):175–85.
40. Kearns NA, Iatrou A, Flood DJ, De Tissera S, Mullaney ZM, Xu J, et al. Dissecting the human leptomeninges at single-cell resolution. Nat Commun. 2023;14(1):7036.
41. Macikova I, Perzelova A, Mraz P, Bizik I, Steno J. GFAP-positive astrocytes are rare or absent in primary adult human brain tissue cultures. Biologia. 2009;64(4):833–9.
42. Escartin C, Galea E, Lakatos A, O'Callaghan JP, Petzold GC, Serrano-Pozo A, et al. Reactive astrocyte nomenclature, definitions, and future directions. Nat Neurosci. 2021;24(3):312–25.

43. Dasgupta K, Jeong J. Developmental biology of the meninges. genesis. 2019;57(5):e23288.
44. Como CN, O'Rourke R, Winkler C, Mitchell D, Tran L, Lorberbaum D et al. Meningeal-derived retinoic acid regulates neurogenesis via suppression of Notch and Sox2. Cell reports. 2025;44 (5).
45. Siegenthaler JA, Ashique AM, Zarbalis K, Patterson KP, Hecht JH, Kane MA, et al. Retinoic acid from the meninges regulates cortical neuron generation. Cell. 2009;139(3):597–609.
46. Hao J, Kohler C, van den Dorpel H, Scholl HPN, Meyer P, Killer HE, et al. The extracellular matrix composition of the optic nerve subarachnoid space. Exp Eye Res. 2020;200:108250.
47. Jones HE, Robertson GL, Bodnya C, Romero-Morales A, O'Rourke R, Gama V, et al. Leptomeningeal Neural Organoid Fusions as Models to Study Meninges-Brain Signaling. Stem Cells and Development; 2025.
48. Dorrier CE, Jones HE, Pintarić L, Siegenthaler JA, Daneman R. Emerging roles for CNS fibroblasts in health, injury and disease. Nat Rev Neurosci. 2022;23(1):23–34.
49. Pietilä R, Del Gaudio F, He L, Vázquez-Liébanas E, Vanlandewijck M, Muhl L et al. Molecular anatomy of adult mouse leptomeninges. Neuron. 2023.
50. Hull VL, Wang Y, McDonough J, Zhu M, Burns T, Al Ramel N, et al. Astroglial conditional Slc13a3 knockout is therapeutic in murine Canavan leukodystrophy. Ann Clin Transl Neurol. 2024;11(4):1059–62. PubMed PMID: 38282243. PMCID: PMC11021635. Epub 20240128. eng.
51. Li Y, Chen Y, Tan L, Pan JY, Lin WW, Wu J, et al. RNA i-mediated ephrin-B2 silencing attenuates astroglial-fibrotic scar formation and improves spinal cord axon growth. CNS Neurosci Ther. 2017;23(10):779–89.
52. Bundesen LQ, Scheel TA, Bregman BS, Kromer LF. Ephrin-B2 and EphB2 regulation of astrocyte-meningeal fibroblast interactions in response to spinal cord lesions in adult rats. J Neurosci. 2003;23(21):7789–800.
53. Niclou SP, Franssen EHP, Ehlert EME, Taniguchi M, Verhaagen J. Meningeal cell-derived semaphorin 3A inhibits neurite outgrowth. Mol Cell Neurosci. 2003;24(4):902–12.
54. Gong CX, Hu LL, Jiang L, Shi PX, Zhang S, Zhao Y, et al. Integrin α8-Mediated Pericyte Morphogenesis Controls Blood-Brain Barrier Integrity. Adv Sci (Weinh). 2025;12(48):e15374. PubMed PMID: 41085070. PMCID: PMC12752560. Epub 20251014. eng.
55. Maître J-L, Heisenberg C-P. Three Functions of Cadherins in Cell Adhesion. Curr Biol. 2013;23(14):R626–33.
56. Nguyen TT, Camp CR, Doan JK, Traynelis SF, Sloan SA, Hall RA. GPR37L1 controls maturation and organization of cortical astrocytes during development. Glia. 2023;71(8):1921–46. PubMed PMID: 37029775. PMCID: PMC10315172. Epub 20230408. eng.
57. Ness R, David S. Leptomeningeal cells modulate the neurite growth promoting properties of astrocytes in vitro. Glia. 1997;19(1):47–57.
58. Heck N, Garwood J, Dobbertin A, Calco V, Sirko S, Mittmann T, et al. Evidence for distinct leptomeningeal cell-dependent paracrine and EGF-linked autocrine regulatory pathways for

suppression of fibrillar collagens in astrocytes. Mol Cell Neurosci. 2007;36(1):71–85.
59. Bocchi R, Thorwirth M, Simon-Ebert T, Koupourtidou C, Clavreul S, Kolf K et al. Astrocyte heterogeneity reveals region-specific astrogenesis in the white matter. Nat Neurosci. 2025:1–13.
60. Beck HN, Drahushuk K, Jacoby DB, Higgins D, Lein PJ. Bone morphogenetic protein-5 (BMP-5) promotes dendritic growth in cultured sympathetic neurons. BMC Neurosci. 2001;2(1):12.
61. Choe Y, Pleasure SJ. Meningeal Bmps regulate cortical layer formation. Brain Plast. 2018;4(2):169–83.
62. Hébert JM, Mishina Y, McConnell SK. BMP signaling is required locally to pattern the dorsal telencephalic midline. Neuron. 2002;35(6):1029–41.
63. Kusakawa Y, Mikawa S, Sato K. BMP5 expression in the adult rat brain. Neuroscience. 2015;284:972–87.
64. Vinsland E, Salas SM, Kapustová I, Hu L, Webb S, Li X et al. Cell atlas of the developing human meninges reveals a dura origin of meningioma. bioRxiv. 2025.
65. Wang AZ, Bowman-Kirigin JA, Desai R, Kang L-I, Patel PR, Patel B, et al. Single-cell profiling of human dura and meningioma reveals cellular meningeal landscape and insights into meningioma immune response. Genome Med. 2022;14(1):49.
66. Santorella E, Balsbaugh JL, Ge S, Saboori P, Baker D, Pachter JS. Proteomic interrogation of the meninges reveals the molecular identities of structural components and regional distinctions along the CNS axis. Fluids Barriers CNS. 2023;20(1):74.
67. Neutzner A, Power L, Dürrenberger M, Scholl HPN, Meyer P, Killer HE, et al. A perfusion bioreactor-based 3D model of the subarachnoid space based on a meningeal tissue construct. Fluids Barriers CNS. 2019;16(1):1–14.
68. Abubaker M. Characterisation of the leptomeningeal cells in vitro under conditions that mimic cerebrospinal fluid flow in healthy and diseased states. 2024.

Figures

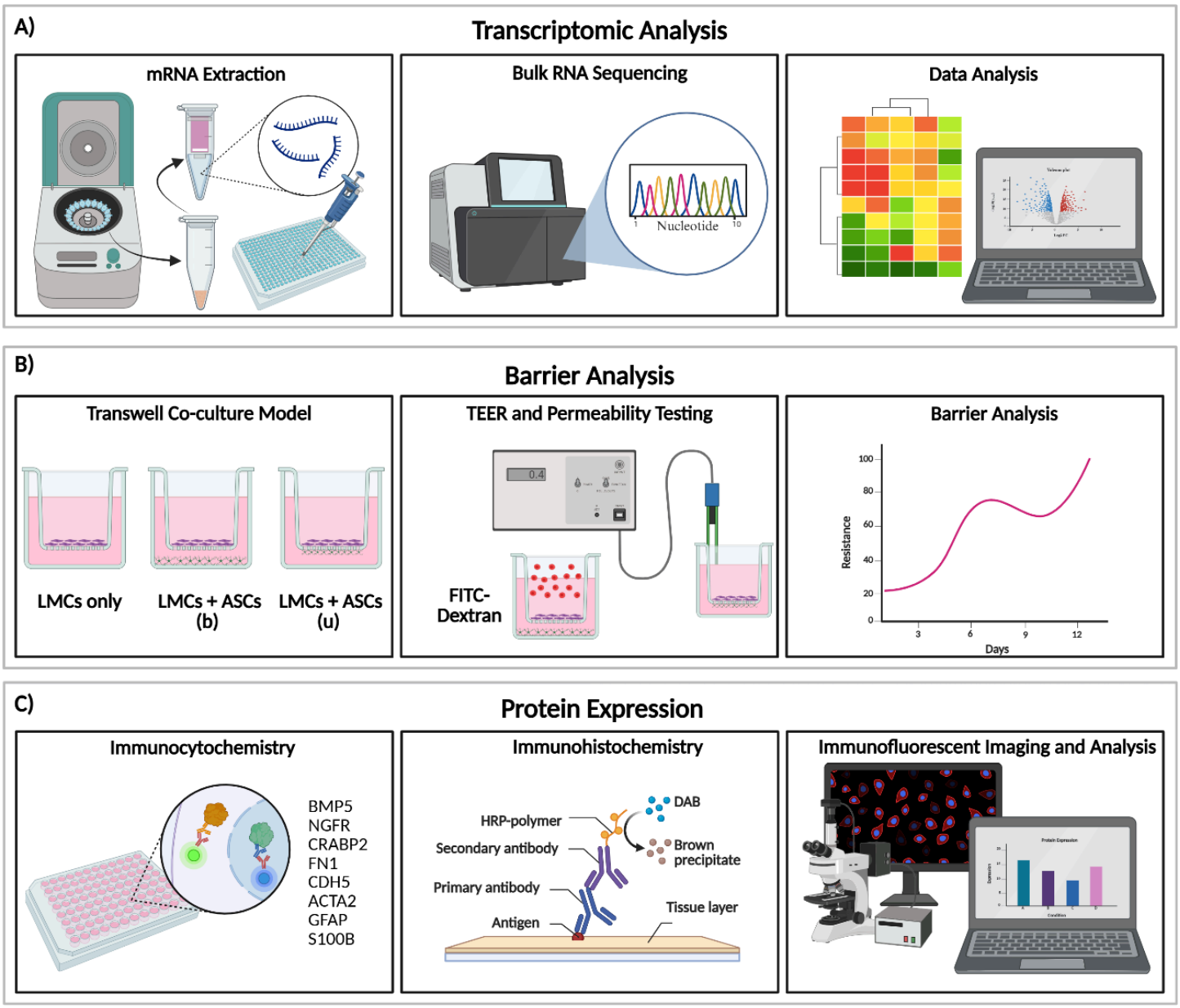

Figure 1

Overview of the methods used in this study. **A)** Bulk RNA sequencing and data analysis **B)** Barrier and permeability analysis done using Transepithelial/Endothelial Electrical Resistance (TEER) and Fluorescein isothiocyanate (FITC)-Dextran using leptomeningeal cells (LMCs) only, LMC + astrocytes (ASCs) (on plate bottom – b), and LMCs + ASCs (on underside of insert – u). **C)** Protein expression using immunocytochemistry and immunohistochemistry.

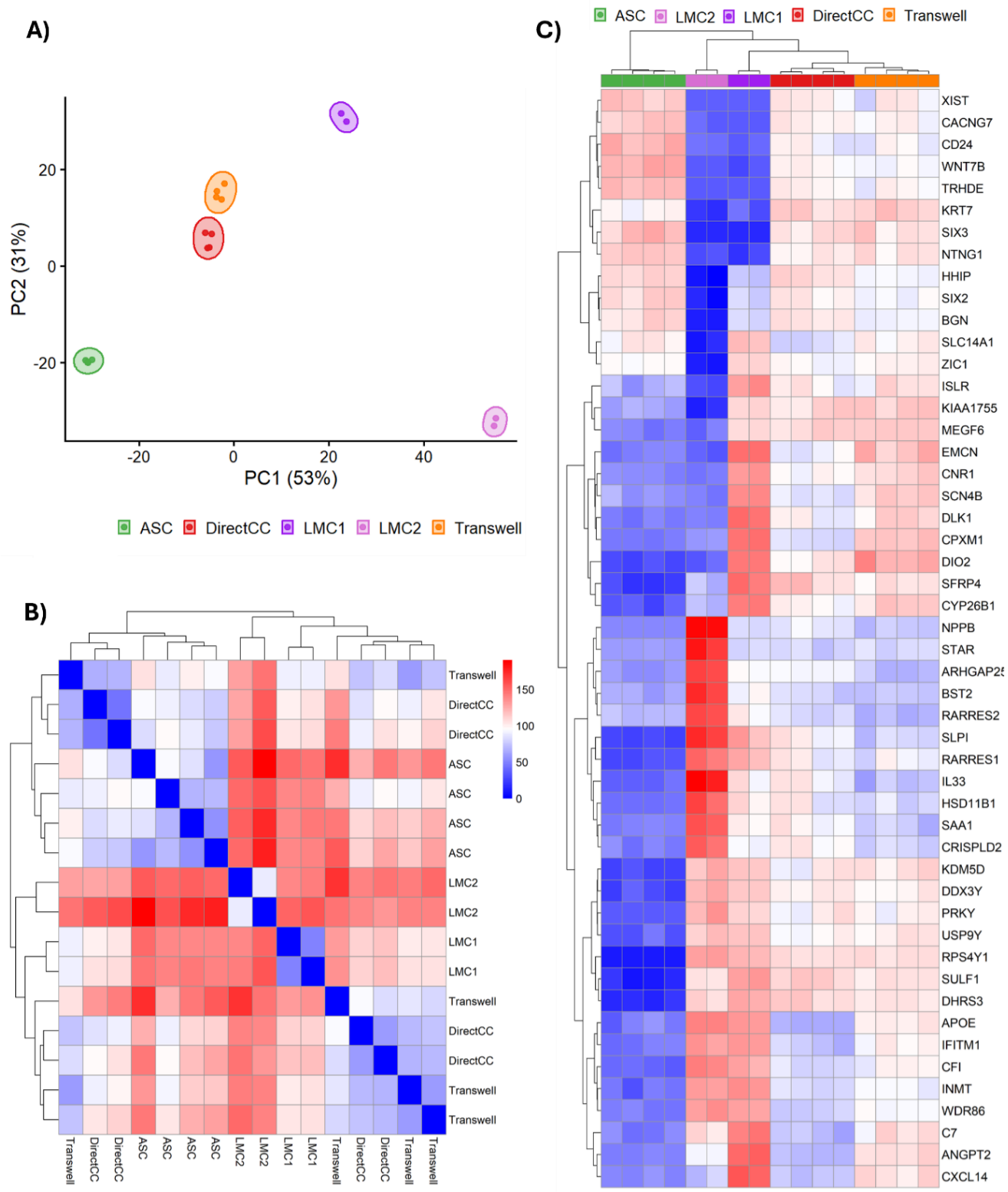

Figure 2

A) Principal component analysis plot for the comparison of gene expression patterns amongst the leptomeningeal cells (LMC1 and LMC2), astrocytes (ASC), direct co-culture of LMC1 and ASC (DirectCC), and Transwell co-culture of LMC1 and ASC (Transwell). **B)** Sample distances plot displaying the clustering of the conditions. **C)** Expression heatmap showing clustering of the dataset across the 5

conditions based on the top 50 more variable genes, with each columns representing individual samples. Relative gene expression levels are displayed as row-scaled Z-scores of variance-stabilized data.

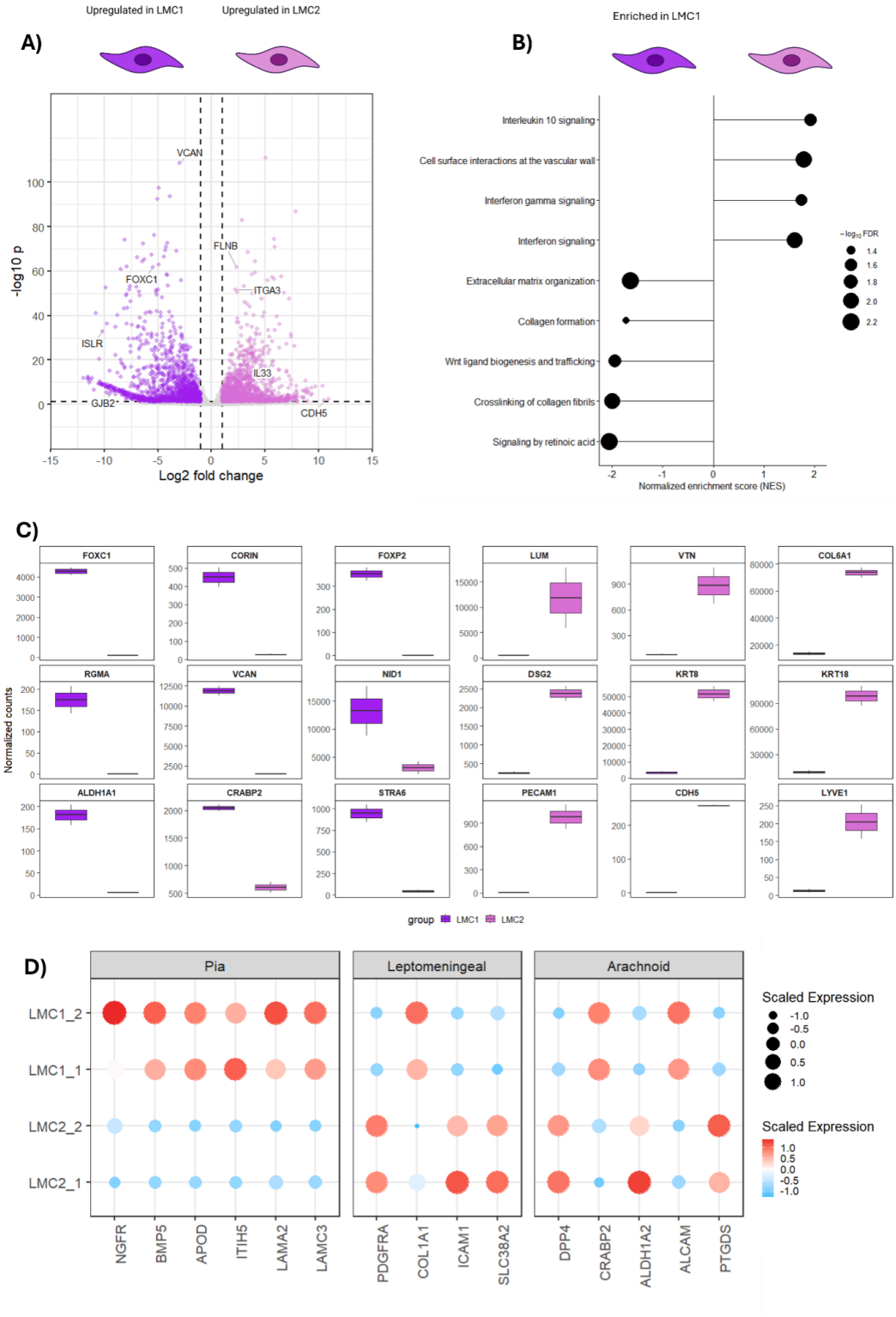

Figure 3

A) Volcano plot of the differentially expressed genes between LMC1 and LMC2 (log2FC>1, padj <0.05) with selected genes of interest highlighted**. B)** Reactome plot of selected terms of interest (padj <0.05)

which are enriched in LMC1 and LMC2. **C)** Boxplots of enriched genes within LMC1 versus LMC2. **D)** Dot plot of pial, general leptomeningeal, and arachnoidal markers to understand the layer specificity of LMC1 and LMC2 (n=2 technical replicates).

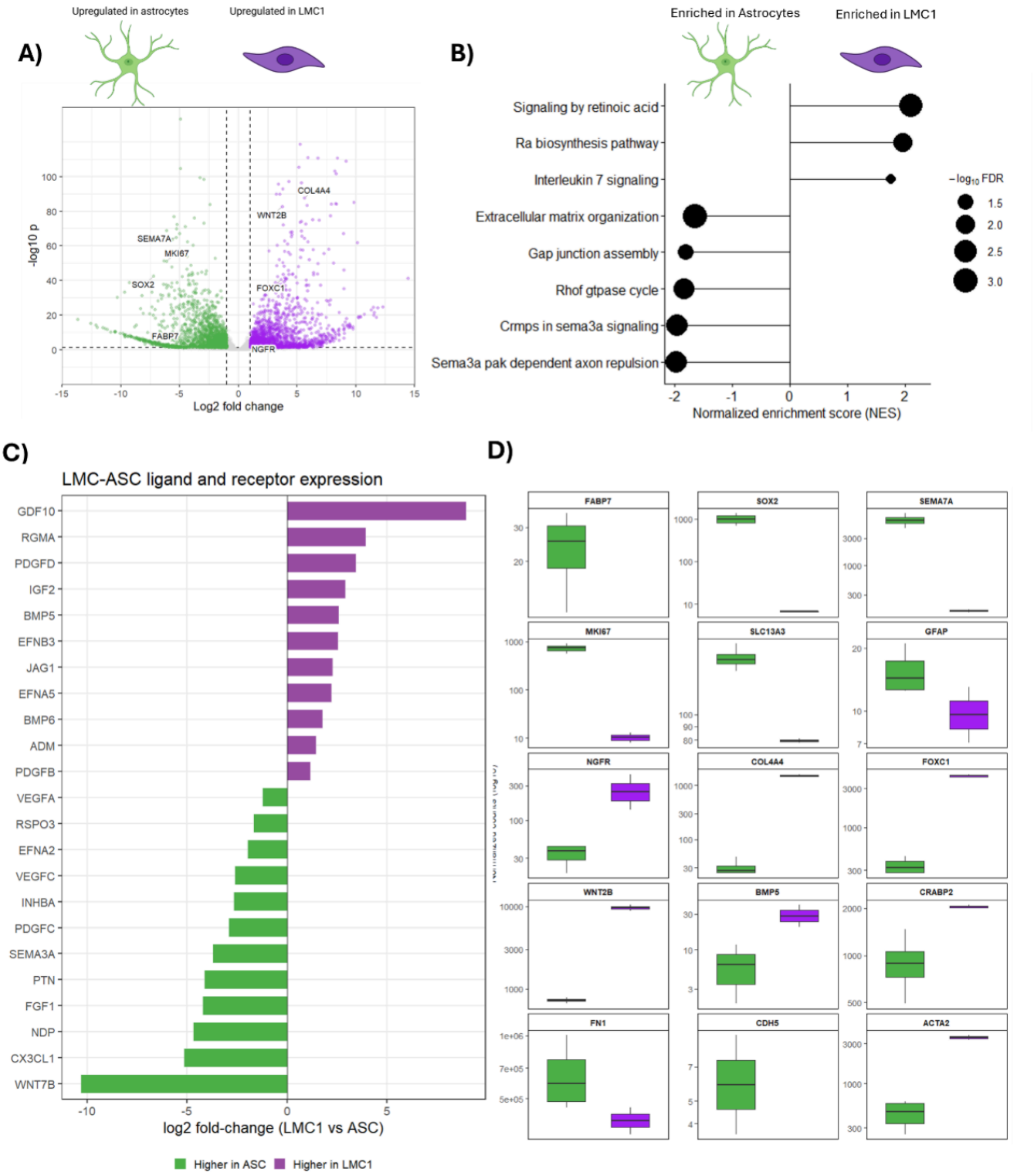

Figure 4

A) Volcano plot of the differentially expressed genes between ASC and LMC1 (log2FC>1, padj <0.05) with top 10 genes highlighted. **B)** Reactome plot of selected terms of interest (padj <0.05) which are enriched in ASC and LMC1. **C)** Boxplot of important LMC and ASC ligand and receptors identified in (29) and their relative expression. **D)** Boxplots of selected genes of interest which were significantly upregulated in LMC1 compared to ASCs.

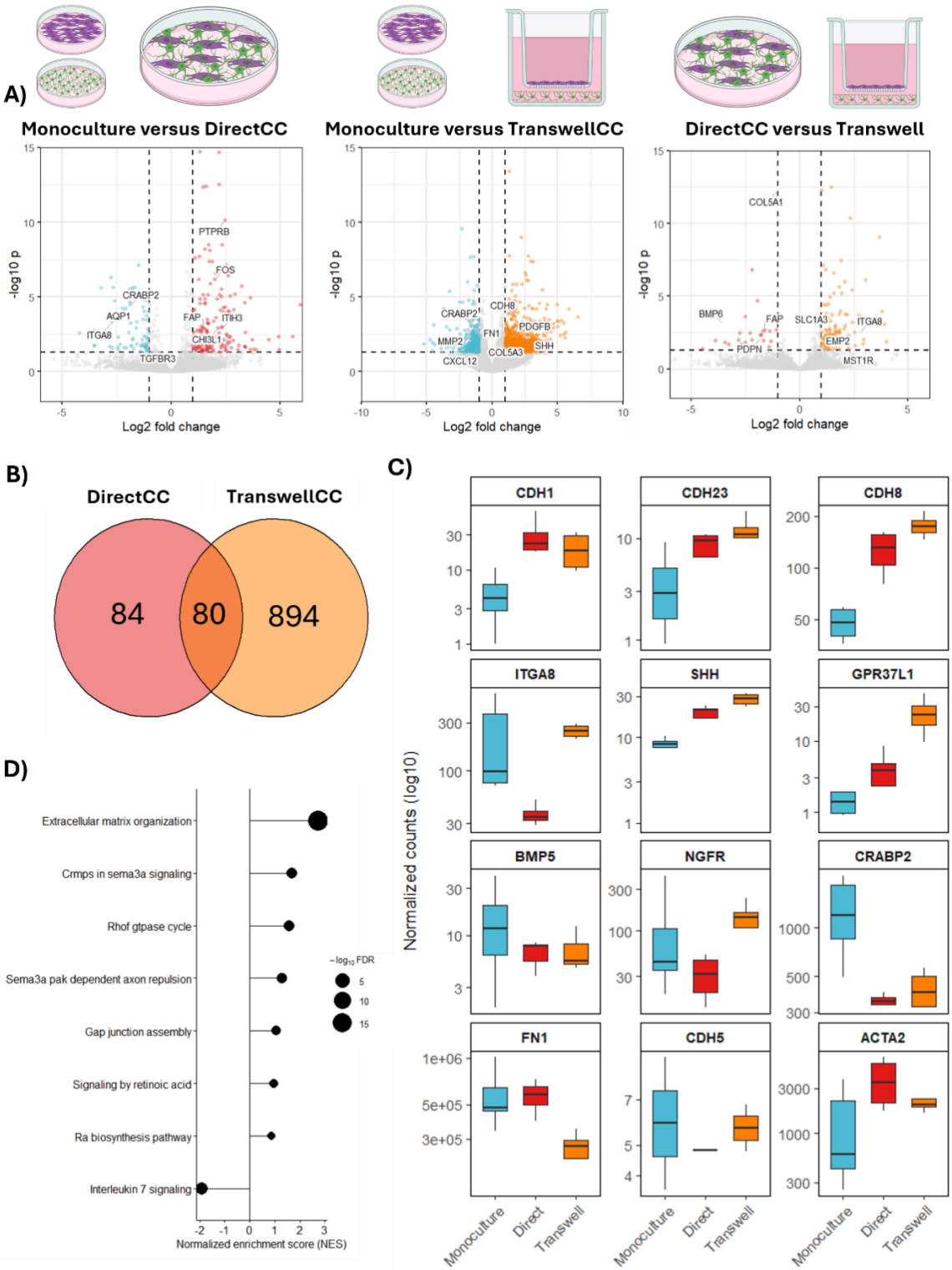

Figure 5

A) Volcano plot of the differentially expressed genes between Monoculture (blue) and DirectCC (red), Monoculture and TranswellCC (orange), and DirectCC and Transwell (log2FC>1, padj.value <0.05) with top genes highlighted. **B)** Venn diagram of the differentially expressed genes in DirectCC and Transwell, along with the shared genes. **C)** Boxplots of selected genes of interest in monoculture, Direct CC, and Transwell. **D)** Reactome pathway enrichment in DirectCC (negative NES score) and Transwell (positive NES).

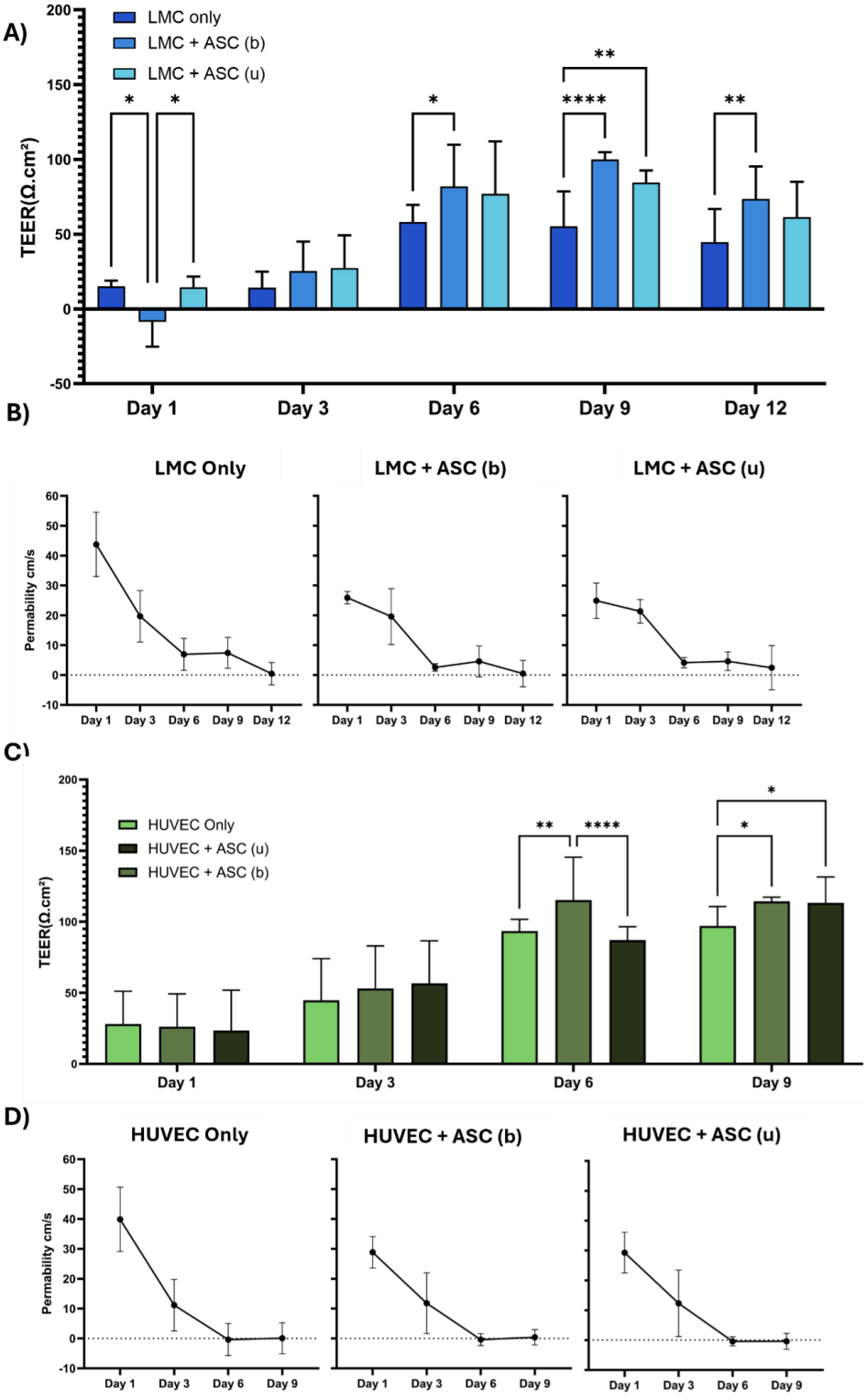

Figure 6

Transendothelial/Transepithelial electrical resistance (TEER) of LMC barrier and HUVECs in the presence and absence of ASCs. **A)** Transendothelial resistance of LMCs only, LMCs +ASC (b), LMCs + ASCs (u) across 12 days. **B)** 4 kDa FITC Dextran permeability assay across 12 days across LMC conditions (cm/s10^6). **C)**Transendothelial resistance of HUVECs only, HUVECs +ASC (b), HUVECs + ASCs (u) across 9 days. **D)** 4kDa FITC Dextran permeability assay across 9 days across HUVECs conditions.

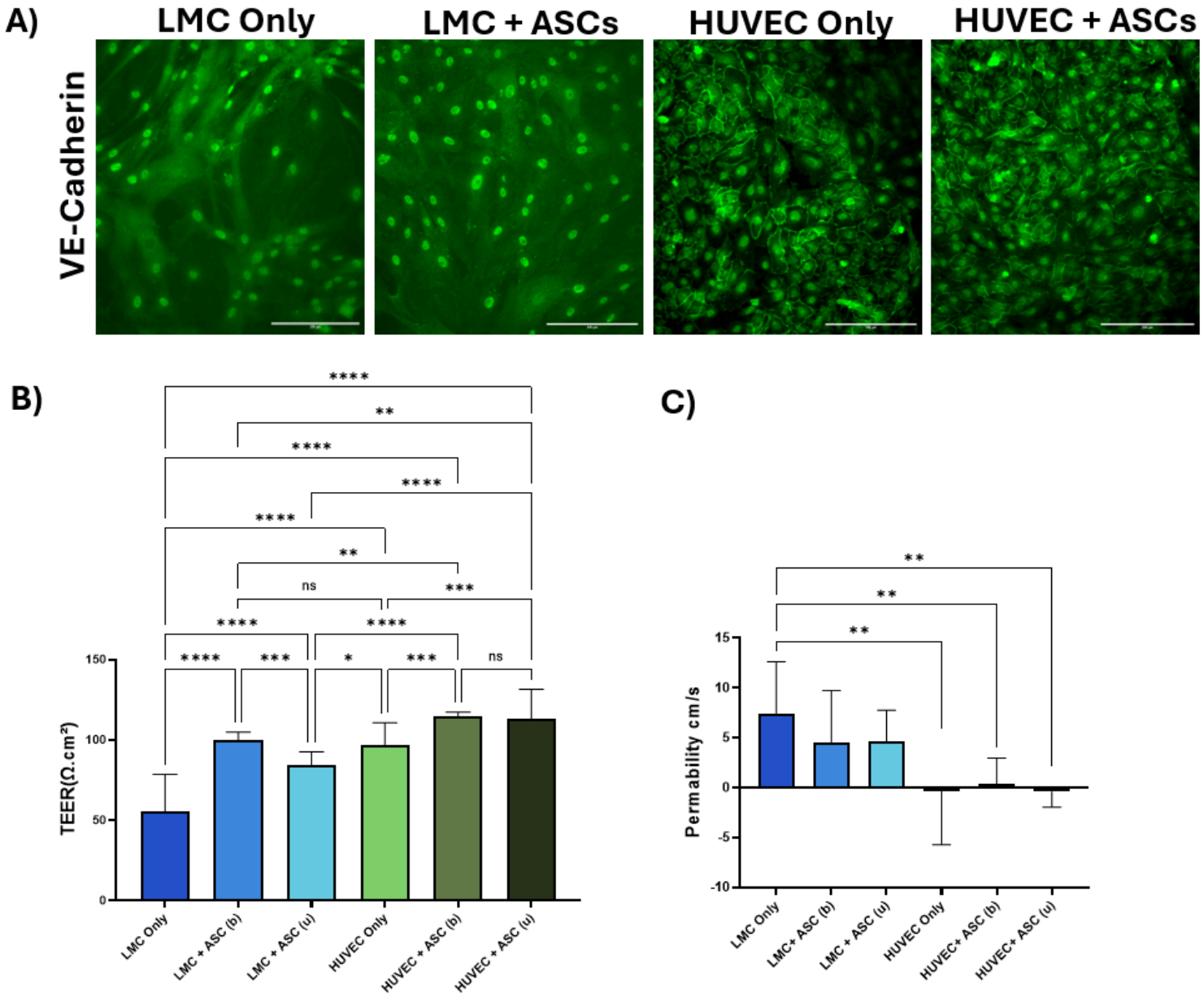

Figure 7

A) Immunocytochemistry of VE-Cadherin across co-culture conditions. Scale bar = 200 µm. **B)** Comparison of TEER values between LMC-ASC and HUVEC-ASC co-culture models. **C)** Comparison of

FITC-Dextran permeability assay between LMC-ASC and HUVEC-ASC co-culture models.

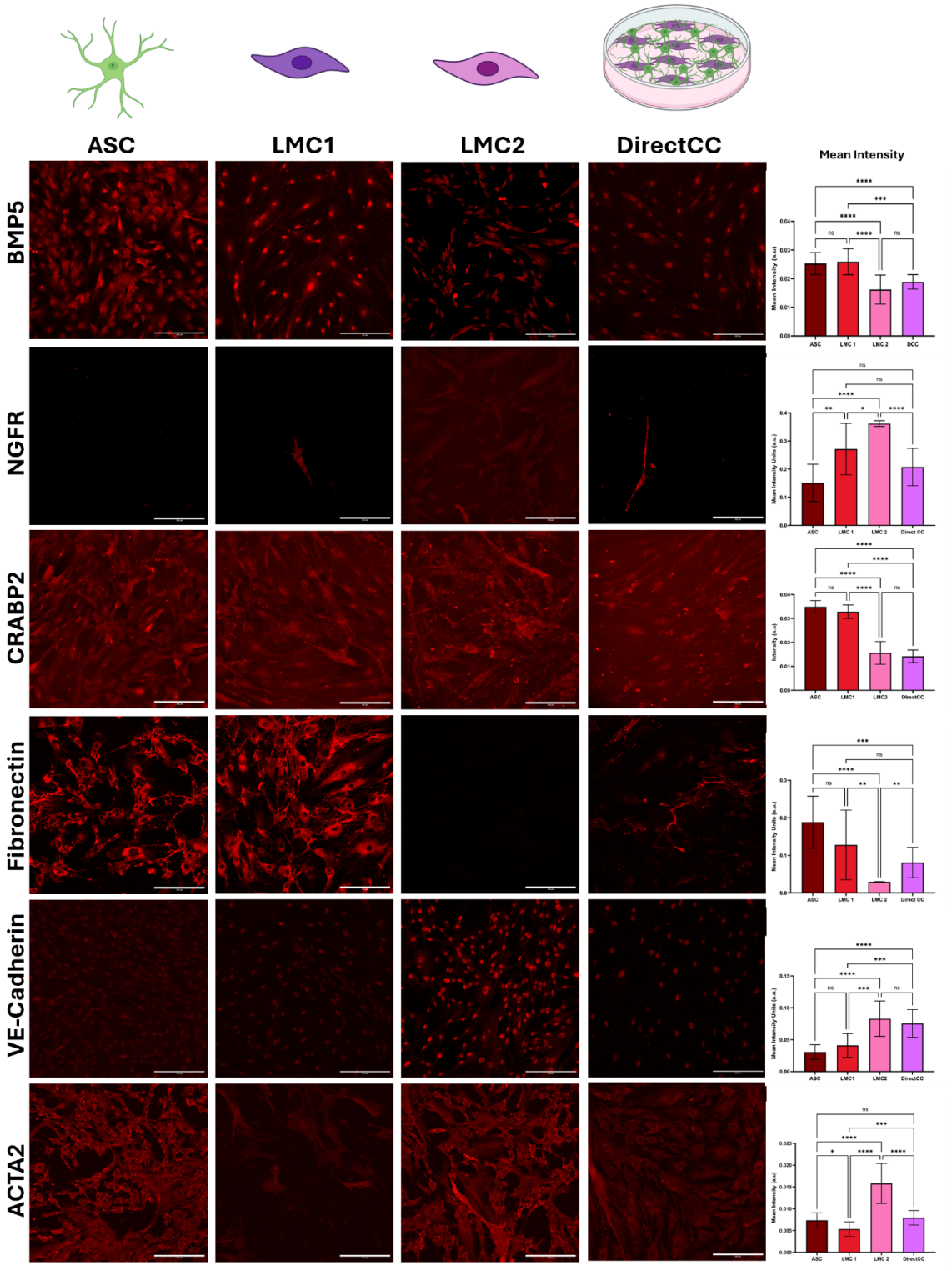

Figure 8

Immunocytochemistry of ASC, LMC1, LMC2, and DirectCC of commonly used leptomeningeal markers – BMP5, NGFR, CRABP2, Fibronectin, VE-Cadherin, ACTA2. Confocal analysis showing representative

images for each condition with accompanying data analysis of overall mean intensity. 15 images per conditions were analysed using Cell Profiler. Scale bar = 200 µm

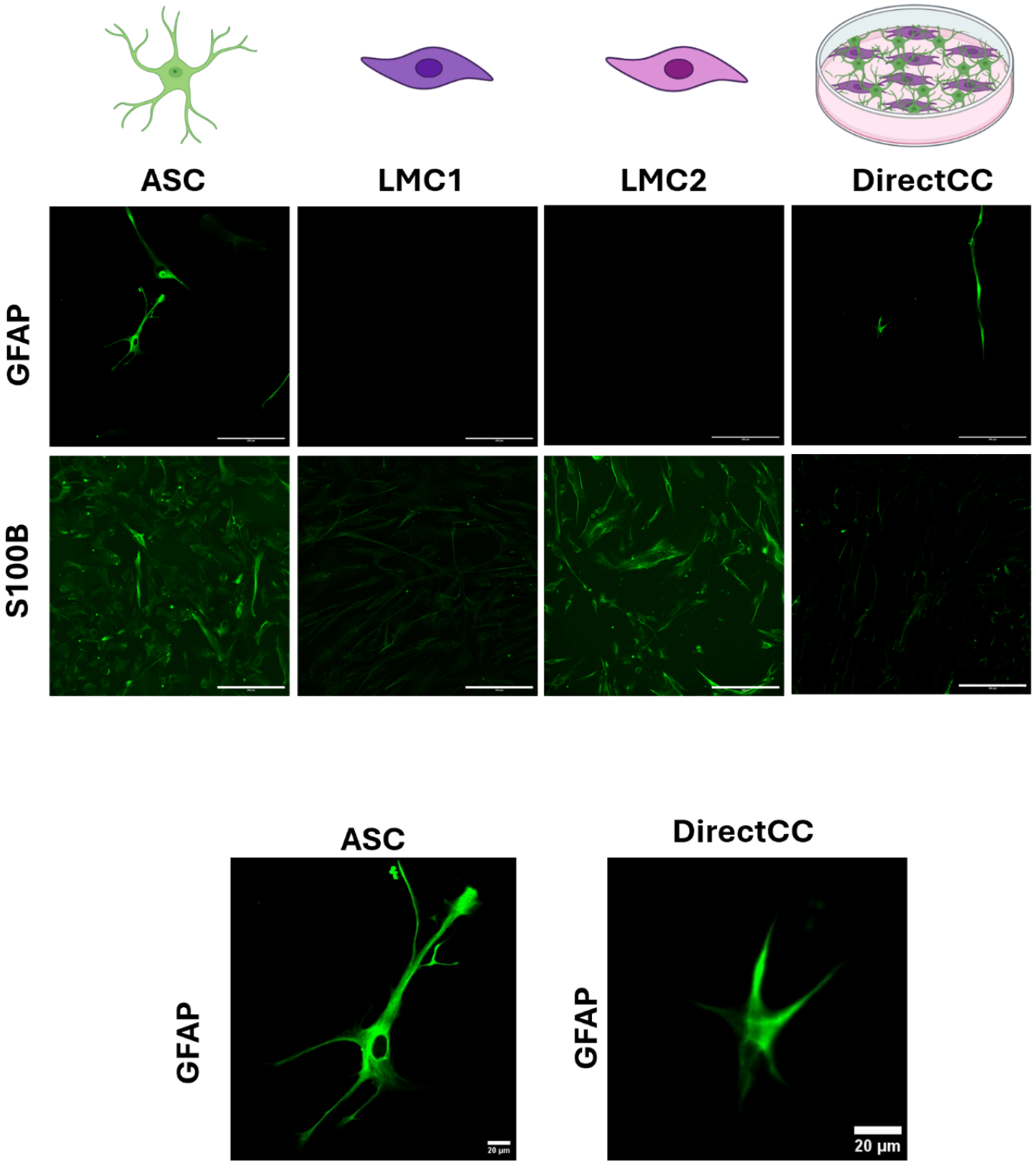

Figure 9

Immunocytochemistry images of astrocyte markers GFAP and S100B across all conditions Scale bar = 200 µm. Below is a zoomed in image of an astrocyte within ASC and DirectCC groups. Scale bar = 20 µm

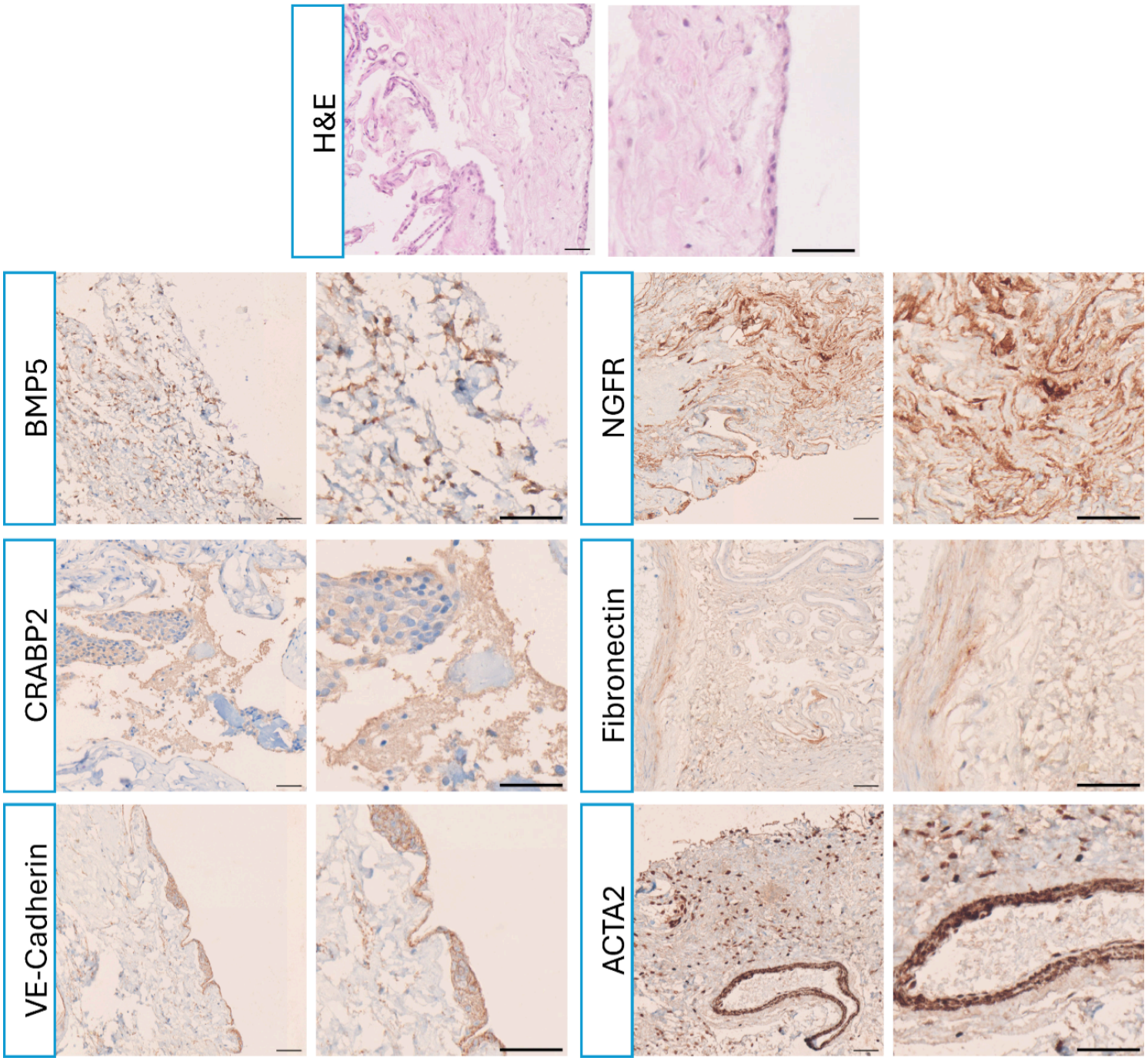

Figure 10

Representative H&E and chromogenic immunohistochemistry of the proteins of interest from FFPE post-mortem adult human meninges n=2 individuals. For each marker, the left image shows a wider field of view, while the right image shows a magnified view of a representative region within the same field. Scale bars = 100 μm.

Supplementary Files

This is a list of supplementary files associated with this preprint. Click to download.

- SupplementaryFile1.docx
- SupplementaryFile2LMC1vLMC2.xlsx
- SupplementaryFile3LMC1vASC.xlsx
- SupplementaryFile4MonocultureversusDirectCC.xlsx
- SupplementaryFile5MonocultureversusTranswell.xlsx
- SupplementaryFile6TranswellverusDirectCC.xlsx
- GA.docx